



Brazilian Journal of Physics

ISSN: 0103-9733

luizno.bjp@gmail.com

Sociedade Brasileira de Física

Brasil

Bernui, Armando

The Large-Scale Angular Correlations in CMB Temperature Maps

Brazilian Journal of Physics, vol. 35, núm. 4B, december, 2005, pp. 1185-1190

Sociedade Brasileira de Física

São Paulo, Brasil

Available in: <http://www.redalyc.org/articulo.oa?id=46435747>

- How to cite
- Complete issue
- More information about this article
- Journal's homepage in redalyc.org

redalyc.org

Scientific Information System

Network of Scientific Journals from Latin America, the Caribbean, Spain and Portugal

Non-profit academic project, developed under the open access initiative

The Large-Scale Angular Correlations in CMB Temperature Maps

Armando Bernui

Instituto Nacional de Pesquisas Espaciais

Divisão de Astrofísica

Av. dos Astronautas 1758,

12227-010 – São José dos Campos, SP, Brazil

(Received on 18 October, 2005)

Observations show that the Cosmic Microwave Background (CMB) contains tiny variations at the 10^{-5} level around its black-body equilibrium temperature. The detection of these temperature fluctuations provides to modern Cosmology evidence for the existence of primordial density perturbations that seeded all the structures presently observed. The vast majority of the cosmological information is contained in the 2-point temperature function, which measures the angular correlation of these temperature fluctuations distributed on the celestial sphere. Here we study such angular correlations using a recently introduced statistic-geometrical method. Moreover, we use Monte Carlo simulated CMB temperature maps to show the equivalence of this method with the 2-point temperature function (best known as the 2-Point Angular Correlation Function). We also investigate here the robustness of this new method under possible divisions of the original catalog-data in sub-catalogs. Finally, we show some applications of this new method to simple cases.

I. INTRODUCTION

According to modern Cosmology, in the primordial Universe ionized barionic matter and photons were tightly coupled until the recombination epoch when the hydrogen and helium nuclei hold their electrons to form neutral atoms, leaving photons to freely stream toward us. These photons, nowadays observed as a faint residual relic radiation termed the Cosmic Microwave Background Radiation (CMB), have a well described black-body Planckian spectrum as the FIRAS instrument on the COBE satellite showed in 1992 (see e.g. [1] and references therein).

Besides this thermal equilibrium feature, the CMB preserved evidences of small variations in temperature (or intensity) from one part of the microwave sky to another, for this called CMB temperature fluctuations (also known as CMB *anisotropies* in the literature), which are interpreted as being originated during their interaction with the primordial matter-density fluctuations. Since at that time the density fluctuations were correlated at specific angular scales characteristic of the physical processes involved (e.g., [2, 3]), such correlations were imprinted in the angular distribution of the the CMB temperature fluctuations. This fact turns of fundamental importance the study of the CMB angular correlations, in order to understand the evolution of the matter-density fluctuations to form the structures –like galaxies and galaxy clusters– observed today.

In the last decades, especially after the COBE mission, observational cosmology evolved astonishingly fast, in such a way that there has been an increasing improvement in the quality of measuring the CMB temperature fluctuations. While with COBE data the CMB studies were restricted to large angular-scales, with the highly precise and excellent angular resolution of WMAP data, analysis at all angular-scales are now possible.

In what follows we present the basics of a recently proposed *method* suitable for the study of the angular correlations in the sky distribution of cosmic objects. Our main interest is focussed in CMB data like those released by the WMAP satel-

lite [4], for this we shall apply the method to CMB temperature fluctuations maps (briefly **CMB maps**), and also investigate the robustness of the method under possible partitions of the original data in sub-catalogs. Finally, we shall show the equivalence of our method with the 2-Point Angular Correlation Function (2-PACF), and this will be done both in a theoretical way using the definitions of these approaches as well as in a computational way using Monte Carlo simulated CMB maps.

II. THE PASH METHOD

Recently, Bernui & Villela [5, 6] introduced a new method to scrutiny the angular correlations in the distribution of cosmic objects in the celestial sphere.

Given a catalog with n cosmic objects (sharing common physical properties), the method consists in first calculate the $n(n-1)/2$ angular distances of all pairs-of-objects and then construct the normalized histogram of the number of pairs with a given angular separation *versus* their angular separation. The Expected-PASH (EPASH) is the histogram obtained for the ideal distribution case. The difference between the PASH, calculated from the observational data, and the EPASH can reveal significant departures of the former histogram with respect to the later, if the signal-to-noise ratio is sufficiently large. This geometric-statistical tool is called the Pair Angular Separation Histogram (PASH) method.

Catalogs with a large number of objects, as high-resolution CMB maps, can be suitable divided in a set of comparable sub-catalogs, provided that they contain a similar number of objects sharing analogous physical properties, i.e. positive and negative CMB temperature fluctuations are not in the same sub-catalog. After the partition of the original catalog in, say K , sub-catalogs one performs a PASH with each one of these sub-catalogs and average them to obtain the Mean-PASH (MPASH). As we shall see below, the MPASH function is independent of the number of sub-maps K in which the original map is divided, provided that the minimum number is $K_{\min} = 2$: one sub-map for the positive CMB and the other for

the negative ones. Finally we perform, and plot, the difference between the MPASH and the EPASH.

The method has the advantage that it does not depend on cosmological parameters or data other than the angular position in the celestial sphere of the cosmic objects listed in the catalog to be analysed. The method is also applicable to incomplete sky maps, including disconnected regions, on condition that the EPASH was obtained under similar characteristics (i.e. the same number of objects per catalog, and where objects are located in the same patch of the celestial sphere). Notice that the WMAP CMB maps do not include the monopole and dipole contributions, therefore for such data the EPASH has to be obtained taking into account these features.

We firstly describes the basics of the method by showing how to obtain a PASH given a catalog of data. A catalog C is a list of n cosmic objects containing their angular coordinates on the celestial sphere and information about their physical properties; here we assume that the objects of a given catalog have common physical properties.

We divide the interval $(0, 180^\circ]$ in N_{bins} bins of equal length $\delta\gamma = 180^\circ/N_{bins}$, where each sub-interval has the form $J_i = (\gamma_i - \frac{\delta\gamma}{2}, \gamma_i + \frac{\delta\gamma}{2}]$, $i = 1, 2, \dots, N_{bins}$, with center in $\gamma_i = (i - \frac{1}{2})\delta\gamma$. Next, we calculate the $N \equiv n(n-1)/2$ angular distances corresponding to the distances between all pairs-of-objects. We denote by $\varphi(\gamma)$ the number of pairs of objects in C separated by a distance $\gamma \in (0, 180^\circ]$. Then,

$$\Phi(\gamma_i) = \frac{1}{N\delta\gamma} \sum_{\gamma \in J_i} \varphi(\gamma), \quad (1)$$

is the normalized counting of the number of pairs of objects, i.e. $\sum_{i=1}^{N_{bins}} \Phi(\gamma_i) \delta\gamma = 1$, separated by an angle γ_i , that lies in the sub-interval J_i .

Let p, q any two objects $p, q \in C$, with angular coordinates $(\theta_p, \phi_p), (\theta_q, \phi_q)$, respectively, where $\theta_p, \theta_q \in [0, 180^\circ]$ and $\phi_p, \phi_q \in [0, 360^\circ]$. The unit vectors \vec{n}_p, \vec{n}_q (i.e., $|\vec{n}_p| = |\vec{n}_q| = 1$) denote the position of the two objects p, q on the celestial sphere. We denote by $\rho(\vec{n}_p)$ the probability densities of the objects distributed on the celestial sphere S^2 and listed in C . Then, the probability density that two objects $p, q \in C$ be separated an angular distance $\gamma \in [0, 180^\circ]$ is defined by

$$\mathcal{P}(\gamma) \equiv \int \int d\Omega_p d\Omega_q \rho(\vec{n}_p) \rho(\vec{n}_q) \delta(\gamma - \hat{d}(\vec{n}_p, \vec{n}_q)), \quad (2)$$

where δ is the Dirac-delta, and $\hat{d}(\vec{n}_p, \vec{n}_q) = \arccos[\cos\theta_p \cos\theta_q + \sin\theta_p \sin\theta_q \cos(\phi_p - \phi_q)]$. Hence, the PASH is simply defined by

$$\Phi(\gamma_i) \equiv \frac{1}{\delta\gamma} \int_{J_i} \mathcal{P}(\gamma) d\gamma. \quad (3)$$

However, if the interval J_i is small enough (as shall be considered here), a suitable approximation for the PASH is

$$\Phi(\gamma_i) \simeq \mathcal{P}(\gamma_i). \quad (4)$$

Notice that $\rho(\vec{n}_p) d\Omega_p$ is the probability of the object p to be in the sky patch $d\Omega_p \in S^2$. Of course, the probability of finding

p in the whole S^2 should be equal to 1,

$$\int_{S^2} \rho(\vec{n}_p) d\Omega_p = 1.$$

Thus, a purely isotropic and normalized density distribution of objects observed in the full-sky S^2 , reads $\rho(\vec{n}_p) = \frac{1}{4\pi}$. With this information, a direct calculation in eq.(2) gives,

$$\mathcal{P}_{\text{full-sky}}^{\text{Expected}}(\gamma) = \frac{1}{2} \sin \gamma, \quad (5)$$

is the EPASH for the case of isotropically distributed objects on the full-sky S^2 .

Notice that a PASH $\mathcal{P}(\gamma)$ satisfies the normalisation property: $\int_0^{180^\circ} \mathcal{P}(\gamma) d\gamma = 1$, which let us to perform the mean of an arbitrary number of histograms, for sub-catalogs containing comparable number of objects. This is a very useful condition since produces a sort of *normalisation* of our method in the sense that *area* of the function MPASH-minus-EPASH is zero:

$$\int_0^{180^\circ} (\mathcal{P}^{\text{MPASH}}(\gamma) - \mathcal{P}^{\text{EPASH}}(\gamma)) d\gamma = 0. \quad (6)$$

III. THE 2-POINT ANGULAR CORRELATION FUNCTION

The Two-Point Angular Correlation Function (2-PACF) is defined by

$$C(\gamma) \equiv \langle T(\vec{n}_p) T(\vec{n}_q) \rangle, \quad (7)$$

where \vec{n}_p, \vec{n}_q are such that $\cos\gamma = \vec{n}_p \cdot \vec{n}_q$, and $T(\vec{n}_p), T(\vec{n}_q)$ are the temperature fluctuations of the pixels p, q of a given CMB map, respectively. Notice that, in some literature (see, e.g. [7]) this definition appears with $T(\vec{n}_p)/T_0$ instead of $T(\vec{n}_p)$, where T_0 is the black-body equilibrium temperature of the CMB. Since $\vec{n}_i, i = p, q$ is a vector with angular coordinates (θ_i, ϕ_i) , $i = p, q$, one can expand $T(\vec{n}_i)$ in the spherical harmonics, so

$$T(\vec{n}_i) = \sum_{\ell m} a_{\ell m} Y_{\ell m}(\theta_i, \phi_i), \quad (8)$$

where $a_{\ell m}$ are the multipole moments, with zero mean $\langle a_{\ell m} \rangle = 0$ for Gaussian temperature fluctuations. In a statistically isotropic Universe the variance of the multipole moments is independent of m , which means that we can define

$$C_\ell \equiv \frac{1}{2\ell+1} \sum_{m=-\ell}^{\ell} |a_{\ell m}|^2, \quad (9)$$

and the set of C_ℓ is termed the angular power spectrum of the CMB map.

Using eqs. (8) and (9), and well-known properties of the spherical harmonics in the definition (7), the 2-PACF for a statistically isotropic Universe can be written as

$$C(\gamma) = \frac{1}{4\pi} \sum_{\ell} (2\ell+1) C_\ell P_\ell(\cos\gamma), \quad (10)$$

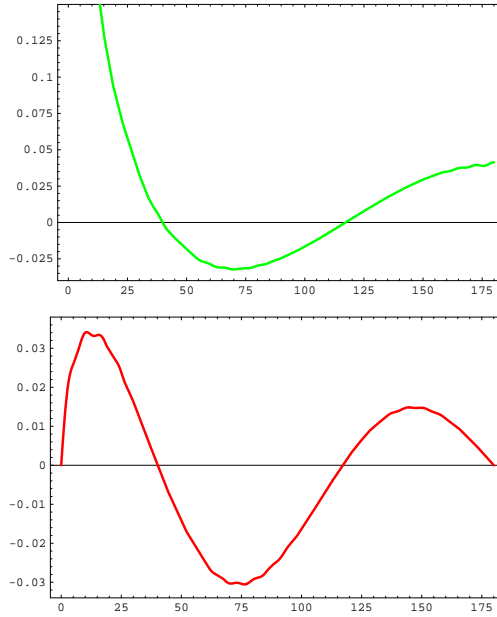


FIG. 1: Here we consider a statistically isotropic Universe with HZ spectrum. Moreover, motivated in WMAP data where the monopole and dipole contributions are not included, here we consider that the sum index starts with $\ell = 2$, i.e. with the quadrupole moment. **Top:** We plotted the 2-PACF, given by $C(\gamma) = \frac{Q}{4\pi} \sum_{\ell=2}^{\infty} \frac{2\ell+1}{\ell(\ell+1)} P_{\ell}(\cos\gamma)$. **Bottom:** We plotted the *normalized* 2-PACF, which defined by $C^{norm}(\gamma) \equiv \frac{\sin\gamma}{2} C(\gamma)$; this 2-PACF is called *normalized* because the area between the curve and the horizontal axis is zero.

where P_{ℓ} are the Legendre polynomial of order ℓ . We define the function

$$C^{norm}(\gamma) \equiv \frac{1}{2} \sin\gamma C(\gamma), \quad (11)$$

and call it the *normalized* 2-PACF because the area between the curve and the horizontal axis is zero, as can be verified from the bottom-plot appearing in Figure 1. Moreover, assuming a Harrison-Zeldovich (HZ) scale-invariant spectrum and for large angular scales (i.e., $\ell \lesssim 100$) we have $C_{\ell} = Q/(\ell(\ell+1))$, where Q is the quadrupole normalisation constant [7, 8]. In Figure 1 we plotted both functions, $C(\gamma)$ and $C^{norm}(\gamma)$, for the case of a statistically isotropic Universe with HS spectrum.

When we use the formula (10), instead of the definition eq. (7), a crucial point appears in the method of the 2-PACF. In fact, intrinsically to the method there is a large uncertainty in the evaluation of the C_{ℓ} 's, called the Cosmic Variance, and is given by $\delta C_{\ell}/C_{\ell} = \sqrt{2/(\ell+1)}$. This reveals no more than our ignorance in determining the real values of the low-order C_{ℓ} (i.e. for $\ell = 2, 3, 4, \dots$).

IV. THE 2-PACF *versus* THE PASH-minus-EPASH FUNCTION

Here we shall prove the equivalence between the PASH method and the 2-PACF.

The above definition of the 2-PACF, eq. (7), can also be written as (see [8], pag. 195, eq. (5.28), where $\xi(\mathbf{x}) = \xi(\cos\gamma) \equiv C(\gamma)$)

$$C(\gamma) + 1 = A \int d\Omega_q \rho(\vec{n}_q) \int d\Omega_p \rho(\vec{n}_p) \delta(\cos\theta_p - \cos(\gamma + \theta_q)) \delta(\phi_p - \phi_q),$$

where A is a constant, and δ is the Dirac-delta. Multiplying both sides by $\frac{\sin\gamma}{2}$, which according to eq. 5 is the EPASH for the full-sky catalog, and using properties of the Dirac-delta we obtain

$$\begin{aligned} & \frac{\sin\gamma}{2} C(\gamma) + \frac{\sin\gamma}{2} \\ &= A \int d\Omega_q \rho(\vec{n}_q) \int d\Omega_p \rho(\vec{n}_p) \delta(\theta_p - \theta_q - \gamma) \delta(\phi_p - \phi_q), \end{aligned}$$

which means that when $\phi_p = \phi_q$, then $\gamma = \theta_p - \theta_q$; in other words the only contribution to the integral comes from the equality $\gamma = \hat{\mathbf{d}}(\vec{n}_p, \vec{n}_q)$. This implies that the right-hand-side of this equation is equal to the definition of the PASH, eq. (2), except for the constant A . Thus, choosing suitably the value of A , we formally obtain the equivalence between both approaches

$$\frac{\sin\gamma}{2} C(\gamma) = \mathcal{P}^{MPASH}(\gamma) - \mathcal{P}^{EPASH}(\gamma).$$

Moreover, we also performed here a computational verification of this equivalence. For this, we carry out the average of 1000 MPASH-minus-EPASH functions from an equal number of Monte Carlo CMB full-sky maps generated under the statistical isotropy and HZ spectrum assumptions. Our results, observed in Figure 2, show the excellent coincidence between both functions which is a computational verification of the equivalence between the MPASH-minus-EPASH function and the *normalized* 2-PACF.

Therefore, we conclude that the two approaches, the MPASH-minus-EPASH and the *normalized* 2-PACF ($C^{norm}(\gamma) = \frac{\sin\gamma}{2} C(\gamma)$) are equivalent. However, it is worth to mention here that the *normalized* version of the 2-PACF seems to be more suitable than the original 2-PACF version, because it leads to scrutiny the angular correlations at all angular scales. As observed in the top-plot of Figure 1, the original 2-PACF is not well-defined for small angular scales $[0, \sim 20^\circ]$.

V. ROBUSTNESS OF THE MPASH CALCULATION

Here we shall study the robustness in the obtention of the MPASH, in the case that it could be obtained considering different partitions (or ways to generate the sub-catalogs) of the original catalog (e.g. the temperature data in a CMB map). We shall deal with this problem by directly showing our results of calculating the MPASH in different partitions (different number of sub-catalogs K) of a given WMAP CMB temperature map.

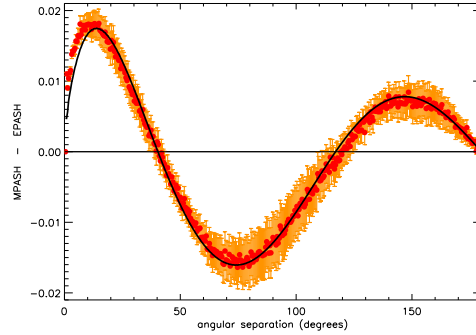


FIG. 2: The red-points (including the standard deviation bars at 1σ) correspond to average of 1000 MPASH-minus-EPASH functions from Monte Carlo CMB maps generated under the statistical isotropy assumption, and the black-line corresponds to the *expected* 2-PACF $C^{\text{norm}}(\gamma) = \frac{\sin \gamma}{8\pi} \sum_{\ell=2} \frac{2\ell+1}{\ell(\ell+1)} P_{\ell}(\cos \gamma)$ for a statistically isotropic Universe. We realize that the excellent coincidence between both results is a validation of the equivalence between the MPASH-minus-EPASH function and the *normalized* 2-PACF.

A CMB full-sky map is the celestial sphere partitioned in a set of equal-area pixels, where to each pixel is assigned a temperature value; so the above mentioned physical property is the CMB temperature fluctuation value of each pixel. To obtain the angular correlations of a CMB map, we order the set of pixels according to increasing values of the pixels temperature. Next, we divide this ordered set of pixels in K disjoint sub-sets (termed sub-catalogs), all of them with a comparable number of pixels. Afterward, we compute the MPASH averaging the K PASHs calculated from each of the K sub-catalogs. As we shall show in Figure 6, the MPASH function is independent of the number of sub-catalogs K in which the original map is divided, provided that the minimum number is $K_{\min} = 2$: one sub-map for the positive CMB and the other for the negative ones. However, it is clear that we can divide the original data in several ways, always following these criteria.

Here we consider the CMB map obtained using WMAP data, specifically the co-added Q+V+W map [9], which is a weighted combination of the 8 high frequency differencing assemblies (DA): Q1, Q2, V1, V2, W1, W2, W3, and W4 (see: http://lambda.gsfc.nasa.gov/product/map/current/IMaps_cleaned.cfm), that is obtained according to

$$T_{\text{co-added}} = \frac{\sum_{I=3}^{10} T_I / \sigma_{0,I}^2}{\sum_{I=3}^{10} 1 / \sigma_{0,I}^2},$$

where T_I is the CMB map for the DA I , and $\sigma_{0,I}^2$ is the noise *per* observation for the DA I .

To investigate whether the MPASH function is independent of the number of sub-catalogs K in which the original catalog is divided due to a large amount of pixels, we study first the angular correlations in the North-Galactic and South-Galactic spherical cap regions of 70° of aberture of the co-added WMAP map. Our neat results shown in Figure 3, for

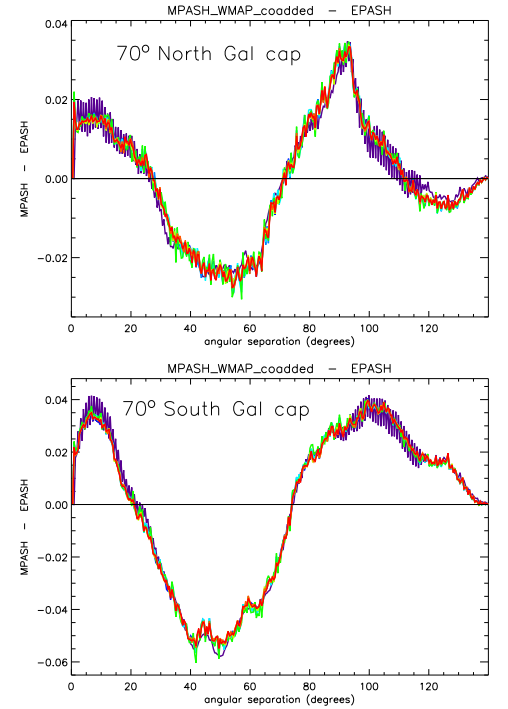


FIG. 3: MPASH-minus-EPASH functions for CMB data in the 70° North and South Galactic spherical caps of the co-added WMAP map [9]. The seven curves plotted in each figure (top and bottom) correspond to the cases where the number of histograms was: $K = 4, 16, 17, 20, 25, 40$, and 80 , respectively. The $K = 4$ case corresponds to the degraded map $N_{\text{side}} = 64$, and all the others to $N_{\text{side}} = 128$ [11]. As observed, the coincidence of this rainbow of curves proves that the MPASH-minus-EPASH is independent of the number K .

the analysis of seven different partitions of the above mentioned regions of the co-added CMB map, demonstrates that the MPASH-minus-EPASH function (and of course also the MPASH) is actually independent of K .

Finally, in Figure 4 we show the same result, but this time for the full-sky WMAP CMB map, termed the ‘cleaned’ map [10], which was produced by combining all the individual frequency WMAP maps using a Wiener filter algorithm in order to reduce or eliminate foregrounds (specially those coming from our Galaxy).

VI. SIMPLE APPLICATIONS OF THE PASH METHOD

In order to illustrate the MPASH-minus-EPASH function revealing signatures in simple cases, here we consider three CMB maps where the angular correlations are known *a priori*:

- a statistically isotropic CMB map, that is there are no angular correlations between the temperature fluctuations of the map; the results of our analysis are shown in Figure 5.

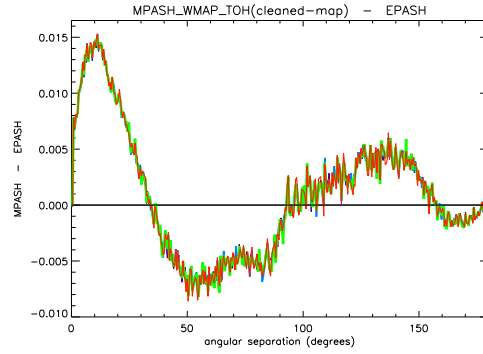


FIG. 4: MPASH-minus-EPASH functions for the full-sky WMAP 'cleaned' map [10]. The four curves plotted here correspond to the cases where the number of histograms to construct the MPASH was: $K = 40, 81, 100$, and 130 , respectively. As observed, all the coloured-curves coincide showing again that the MPASH-minus-EPASH function is independent of the number K .

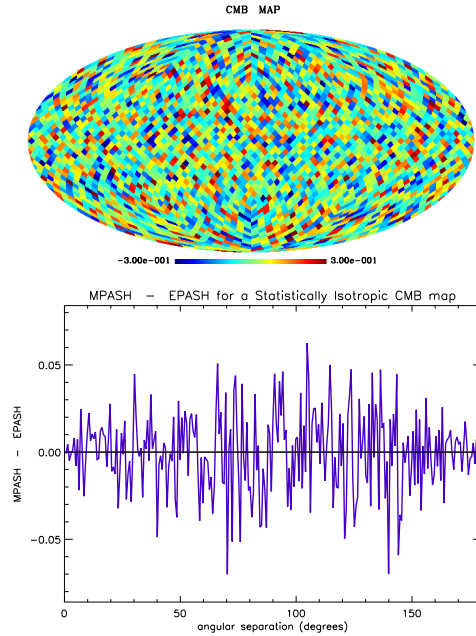


FIG. 5: Statistically isotropic CMB map and the MPASH-minus-EPASH analysis for these data. The MPASH-minus-EPASH function is just a statistical (noisy) oscillations around the horizontal axis, revealing just the absence of angular correlations in the data.

- a pure dipole map; the results of our analysis are shown in Figure 6.
- a pure quadrupole map; the results of our analysis are shown in Figure 7.

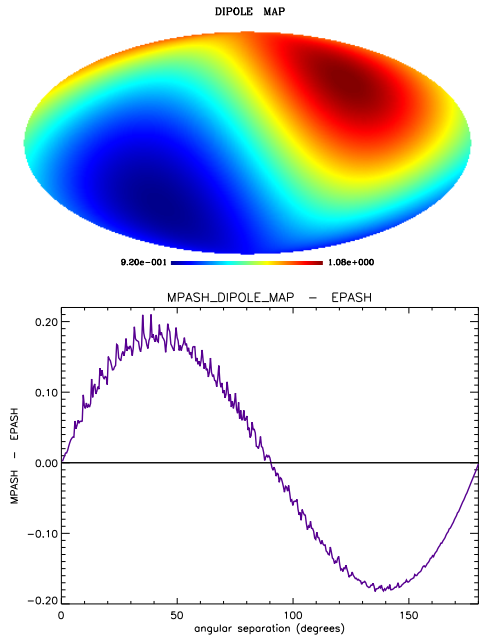


FIG. 6: A CMB Dipole map and the MPASH-minus-EPASH analysis for these data. The MPASH-minus-EPASH function results in a *Sine* function, trivially revealing a typical dipole-signature (with some statistical noise).

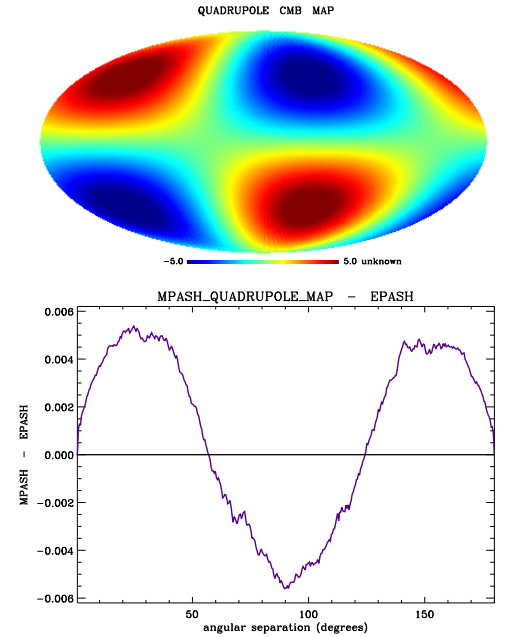


FIG. 7: A quadrupole CMB map and the MPASH-minus-EPASH function resulting from these data. A short analysis of the physical data let us to realize that this function actually represents a quadrupole angular-correlation signature, again with some level of statistical noise.

Acknowledgements

I acknowledge use of the Legacy Archive for Microwave Background Data Analysis (LAMBDA). Some of the results in this paper have been derived using the HEALPix [11] package. I am grateful to Thyrso Villela for many useful discus-

sions. I am indebted to Carlos Alexandre Wuensche, Rodrigo Leonardi, and Ivan Ferreira for introducing me into the *labyrinth* of the CMB TOOLS and the IDL *mysterious*. I acknowledge also a PCI/7B-CNPq fellowship. Last but not least, my thanks to the Organizers of the Conference 100 YEARS OF RELATIVITY for their kind hospitality.

-
- [1] D. Scott and G. F. Smoot, *astro-ph/0406567* (2004).
 - [2] W. Hu and S. Dodelson, *Annual Review of Astronomy and Astrophysics*, **40**, 171 (2002).
 - [3] W. Hu and M. White, *Sci. Amer.*, Feb, 44 (2004).
 - [4] C. L. Bennett, *et al.* *Astrophys. J. S.* **148**, 1 (2003).
 - [5] A. Bernui and T. Villela, *astro-ph/0511339*, to appear in *A&A* (2005).
 - [6] A. Bernui, T. Villela, and I. Ferreira, *Int. J. Mod. Phys. D*, **13**, 1189 (2004).
 - [7] M. Bersanelli, D. Maino, and A. Mennella, 'Anisotropies of the cosmic microwave background', *Rivista del Nuovo Cimento*, Vol.25, N. 9 (2002).
 - [8] T. Padmanabhan, 'Structure formation in the universe', Cambridge Univ. press, (1993).
 - [9] G. Hinshaw, *et al.*, *Astrophys. J. S.* **148**, 135 (2003).
 - [10] M. Tegmark, A. de Oliveira-Costa, and A. J. S. Hamilton, *Phys. Rev. D*, **68**, 123523 (2003).
 - [11] K. M. Górski, *et al.* *Astrophys. J.*, **622**, 759 (2005).